CELL-INTEGRATED SENSING FUNCTIONALITIES FOR SMART BATTERY SYSTEMS WITH IMPROVED PERFORMANCE AND SAFETY

GA 957273

D2.5- CHARACTERIZATION OF 3-5 CM^2 POUCH CELLS WITH THE INTEGRATED LEVEL-2 SENSOR

LC-BAT-13-2020 - Sensing functionalities for smart battery cell chemistries

Deliverable No.	D2.5	
Related WP	WP2	
Deliverable Title	Characterization of 3-5 cm^2 pouch cells with the integrated level-2 sensor	
Deliverable Date	27-02-2023	
Deliverable Type	REPORT	
Dissemination level	Public (PU)	
Written By	Hossein Beydaghi (BDM) Sebastiano Bellani (BDM) Piera Di Prima (POL) Davide Dessantis (POL)	10-02-2023 10-02-2023 10-02-2023 10-02-2023
Checked by	Silvia Bodoardo (POL) Francesco Bonaccorso (BDM)	14-02-2023 15-02-2023
Reviewed by	Iñigo Gandiaga (IKE)	17-02-2023
Approved by	Iñigo Gandiaga (IKE)	27-02-2023
Status	Final	27-02-2023

Summary

The deliverable D.2.5 "Characterization of 3-5 cm^2 pouch cells with integrated level-2 sensor" and comparison with the standard cell without the printed sensor describes the activities related to the Task 2.5 of the WP2 of SENSIBAT project.

More specifically, Task 2.5 focused on the characterization of the pouch cell with reference electrodes printed on Celgard 2500 separator, as well as without, in terms of potential monitoring, galvanostatic charge-discharge (GCD) cycling and electrochemical impedance spectroscopy (EIS) measurements. The obtained results indicated that the reference electrode marginally affect the performance of the whole pouch cell. The electrochemical characterizations reported in the present deliverable confirm the reliable operation of the produced printed LFP- and LTO-based reference electrodes to monitor the electrodes potential and EIS measurements in Li-ion battery pouch cells without interfering in battery operation. The impedance of each individual half-cell was measured by means of the printed reference electrodes, proving similarity between the sum of the half-cell impedances and the one of the full cells.

This deliverable and the related task do not include any deviation from the objectives and timings planned in the Grant Agreement of the SENSIBAT project.

Table of Contents

List of Figures

List of Tables

Abbreviations

Symbol / Abbreviation	
CC	Constant current
Ch Cap	Charge capacity
CE	Coulombic efficiency
CMC	carboxymethyl cellulose
CV	Cyclic voltammetry
Dch Cap	Discharge capacity
DoD	Depth of Discharge
EC:DEC	ethylene carbonate:diethyl carbonate
EIS	Electrochemical Impedance Spectroscopy
f_C	Characteristic frequency
GCD	Galvanostatic charge-discharge
LFP	Lithium iron phosphate
LTO	Lithium titanate
NMC	Lithium Nickel Manganese Cobalt Oxide
NMC662	$LiNi_{0.6}Mn_{0.2}Co_{0.2}O$
NMP	N-Methyl-2-pyrrolidone
PAA-grafted CCM	Poly(acrylic acid sodium)-grafted carboxymethyl cellulose
PEIS	Potentiostatic electrochemical impedance spectroscopy
PVDF	Polyvinylidene difluoride
R_{CT}	Charge transfer resistance
R_{EL}	Electrolyte resistance
SEI	Solid electrolyte interphase
SLG/FLG	Single-/few-layer graphene
SoC	States of Charge
WJM	Wet-jet milling
Z	Impedance contribution of the mesh and electrolyte in the pores
τ	Characteristic time constant

1 Introduction

The main objective of Task 2.5 of WP2 is the validation of the produced printed reference electrodes (prepared in Task 2.2 and reported in deliverable D2.2) in 3-5 cm^2 pouch Li-ion cells. Once validated, the reference electrodes were printed on Celgard 2500 by screen printing and stencil printing techniques and sent to VAR and ABEE for the assembling of 1Ah prototype cells with integrated level 2 sensing functionalities (WP3, Task 3.5).

To validate the level 2 sensor technology developed in WP2 and described in deliverables D2.2 and D2.3, POL assembled pouch cells using a NMC622 cathode and a graphite anode (electrodes supplied by VAR). Two Celgard 2500 were used as the separators, in each cell. On one of the separators, the optimized sensors, based on lithium titanate (LTO) or lithium iron phosphate (LFP) active materials and wet-jet milling (WJM)-produced single/few-layers graphene (SLG/FLG) flakes (produced by BDM), were printed by screen and stencil printing techniques (see details in deliverable D2.4). Finally, $LiPF_6$ 1M in EC:DEC 1:1 v/v solution was used as electrolyte.

The electrochemical characterizations of two- and three-electrode pouch cells were compared to demonstrate that the insertion of a printed reference electrode does not affect the performance of the full cell. The preconditioning step stabilizes the equilibrium potential of the produced printed reference electrodes to ensure reliable measurements during long-term measurements. Our electrochemical analysis evidenced that the printed reference electrodes are stable for more than 400 hours. The impedance contribution of the reference electrodes (having a thickness of 15 µm) was properly modelled through a mesh-like electrical equivalent circuit. Based on this model, symmetric coin cell configurations were used to calculate the impedance of the reference electrodes. The latter were successfully used to measure the half-cell impedance in pouch cells, as well as to monitor individually the potentials of the cell anode and cathode.

2 Experimental

2.1 Reference electrode fabrication

Two different types of reference electrodes were printed by BDM on Celgard 2500 by screen and stencil printing. The reference electrodes with a polyvinylidene difluoride (PVDF) binder (from a N-Methyl-2-pyrrolidone (NMP)-based paste, as described in previous WP2 deliverables) was deposited by stencil printing, while novel reference electrodes with poly (acrylic acid sodium)-grafted carboxymethyl cellulose (PAA-grafted CMC) binder (from a water-based paste) were produced by screen printing. First, BDM sent the printed reference electrodes (with a size of 2×0.5 cm^2) to POL for the completion of WP2 Task 2.5 activities. Afterwards, BDM also produced 60 reference electrodes (with a size of 5×0.8 cm^2) for VAR and ABEE for the assembling of 1Ah prototype cells with integrated level 2 sensing functionalities (WP3, Task 3.5).

Figure 1a shows the frame for screen printing designed by BDM and used to print the reference electrodes based on PAA-grafted CMC binder with a bench-top semi-automatic screen-printing film coater (EQ-SPC-3050, MTI Corp.). Since the NMP solvent dissolved the photoresist of the frames, stencil masks were designed to produce the reference electrodes with PVDF binder by stencil printing using a blade coater (MSK-AFAH200A, MTI Corp.). Noteworthy, screen-printing deposition technique improved the spatial resolution of the reference electrodes, but BDM has not identified yet a suitable photoresist compatible with NMP. The reference electrode pastes were thus deposited on Celgard 2500 separator and dried at 80 °C for 2 hours under a vacuum oven (Binder, VD 53-UL). Figure 1b shows a representative sample of an LFP-D reference electrode (see composition in deliverable D2.4) printed on Celgard 2500 by screen printing. The electrical resistivity measurements through the four-probe method coupled with contact profilometry has shown an electrical resistivity as low as 0.06 Ω × cm for the produced reference electrodes.

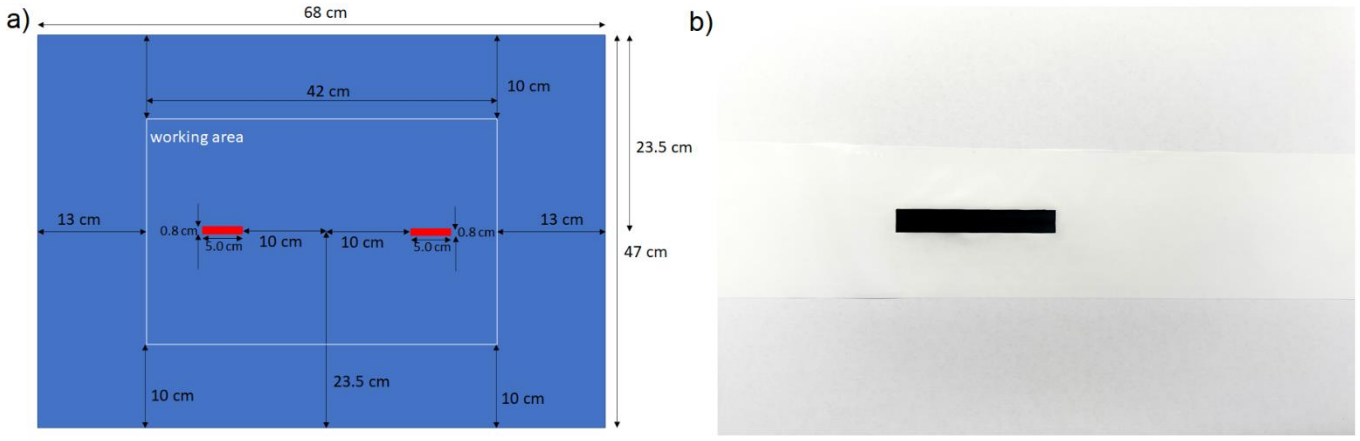

Figure 1. a) Design of frame for screen printing. b) Photograph of a representative sample of LFP-D reference electrode printed on Celgard 2500 by screen printing.

2.2 Two- and three-electrode pouch cells assembly and optimization

For the final characterization of the produced printed reference electrode, either two- and three-electrode pouch cells have been assembled adjusting the procedures described in deliverables D2.2 and D2.3. Two-electrode pouch cells have been produced as reference cell to compare their electrochemical performance with those including the developed printed reference electrode. Kapton HN tape (polyimide sheet with a thickness

of 20 µm) with a 30 µm-thick strapping tape was used to ensure electrical and chemical insulation of the reference electrodes from the electrolyte, as shown in Figure 2a. This tape is based on polypropylene film coated with a specific rubber adhesive featuring a strong resistance to Li-ion battery electrolytes, including LiPF6 EC:DEC 1:1 v/v, as used in the SENSIBAT project. By taking advantage of the new facilities recently installed at POL and including a new battery pilot line, all the assembling procedure was performed in a dry room (dew point -25 °C (@25 °C)). Tabs were welded on the electrodes with an ultrasonic metal welder to guarantee reliable connections. Aluminium tabs (3 mm width) were used for the cathodes and LFP-based reference electrodes, while Nickel tabs (4 mm width) were adopted for the LTO-based reference electrodes and anodes. As described in deliverable D2.4, graphite was used as the anode and NMC622 as the cathode, both provided by VAR. A graphite anode of 2.1 x 1.6 cm2 and a NMC622 cathode of 2.0 x 1.5 cm2 were cut from larger samples according to the target of 3 cm2 pouch cells. The different sizes of the electrodes ensured that the anode covered completely all the cathode surface, avoiding capacity losses caused by slight misalignment of the electrodes during the cell assembly. For the three-electrode pouch cell configurations (Figure 12), LFP-D and LTO-D reference electrodes (see full description of electrode naming and formulation in deliverable D2.2) have been chosen as printed reference electrodes. Both reference electrodes contain an optimized content of active material (65 wt%) that ensures stable equilibrium potential during cell cycling to correctly determines anode and cathode potentials, while permitting reliable EIS measurements of the half-cells. A square of 2 x 2 cm2 of Celgard®2500 covered by a strip of the reference electrode (2 × 0.5 cm2) was placed between the electrodes. A second piece of 2 x 3.5 cm2 of Celgard®2500 was incorporated into the pouch cell atop the reference electrode to avoid the electrical contact between the reference electrode and the cell electrodes. Experimentally, LFP-D and LTO-D reference electrodes were placed facing the graphite anode and NMC622 cathode, respectively. A square of 0.5 × 0.5 cm2 of the reference electrode was covered by the welded tab, and only 1.5 x 0.5 cm2 area of the reference electrodes remained exposed to form the useable active area of the reference electrode. Finally, the two- and three-electrode pouch cells were sealed inside an Ar-filled glove box (MBraun Labstar, H2O and O2 content < 1 ppm). A compact vacuum sealer was used to make vacuum and seal the pouch cell after adding the liquid electrolyte. During cycling, the cells were clamped with a stable pressure (around 1.2 kg/device area) to ensure proper contact between the electrodes and other cell components.

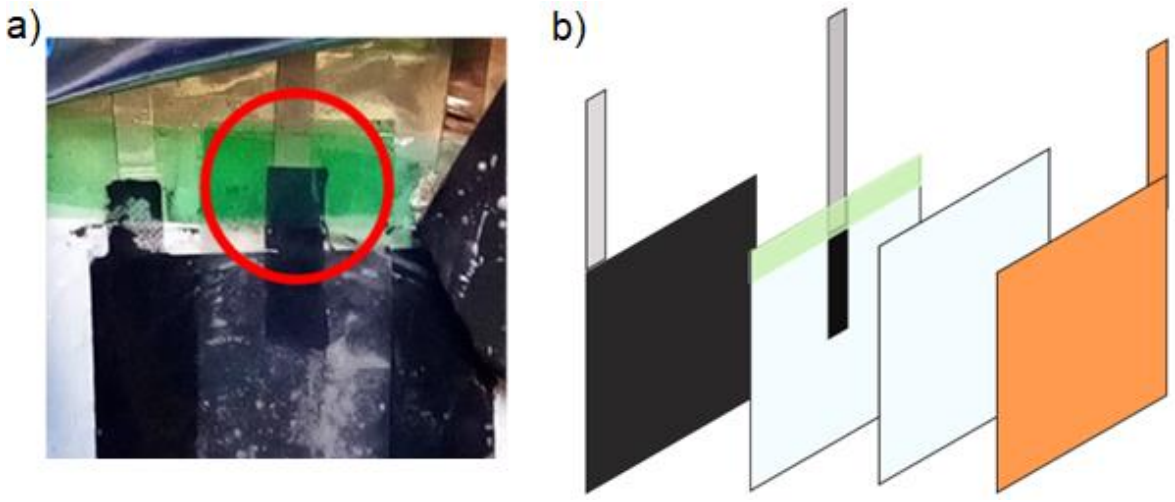

Figure 2. a) Photograph of the three-electrode pouch cell, focusing on the strapping tape and reference electrode regions. b) Sketch of the three-electrode pouch cell configuration. From left to right: NMC622 cathode, reference electrode printed on Celgard 2500, Celgard 2500, graphite anode.

3 Electrochemical tests

3.1 Cyclic voltammetry (CV) analysis of printed reference electrodes

Before the cell assembly, the printed reference electrodes were characterized by cyclic voltammetry (CV) measurements in coin cell CR2032 configuration, using metallic lithium as the counter electrode, Celgard®2500 as a separator soaked by $LiPF_6$ EC:DEC 1:1 v/v, and LFP-D or LTO-D reference electrodes printed on Celgard®2500 as the working electrode. A potential scan rate of 0.1 mV s^{-1} was applied for several cycles in a potential range of 1-3 V and 2-4 V *vs.* Li/Li^+ for LTO-D and LFP-D reference electrodes, respectively. Figure 3 shows the CV curves measured for the investigated reference electrodes, evidencing the oxidation/reduction peaks expected for LTO and LFP at potential around 1.55 V [3] and 3.45 V [4] vs. Li/Li^+, respectively.

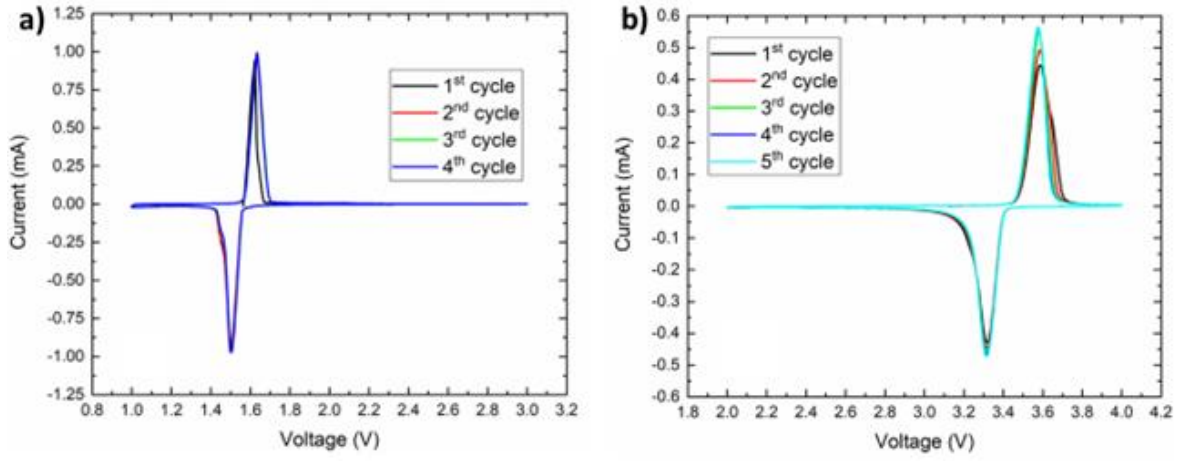

Figure 3. CV curves of the investigated printed reference electrodes: a) LTO-D and b) LFP-D.

3.2 Two- and three-electrode pouch cells characterization

The protocol used for the final electrochemical characterization is the one defined in deliverable D1.2 "Testing plan for cells and modules", coherently modified for the new assembled pouch cell configurations. The protocol composes of five different steps: preconditioning, check-up, reference electrode stabilization, GCD cycling and EIS at different C-rates, and final check-up. The nominal capacity of NMC622, *i.e.*, 2.7 mAh cm^{-2} (as provided by VAR), was used to compute the currents to be used for the pouch cell characterization.

Preconditioning, check-up and final check-up were performed with an Arbin cycler in a two-electrode cell configuration. The reference electrode stabilization, GCD and EIS were performed with a Biologic VMP3 potentiostat in three-electrode cell configuration.

3.2.1 Preconditioning

In this phase, after 24 h from the cell assembly, the pouch cell was cycled at low C-rate (C/10) for 2 GCD cycles, thus adjusting the procedures described in Table 6 of D1.2 to establish comparable starting conditions amongst the cells investigated within the project. Figure 4 shows an example of the preconditioning procedure for a representative two-electrode pouch cell. At C/10, the cell has shown a capacity larger than the nominal one because the latter is computed at higher C-rate (C/2), as clarified by VAR.

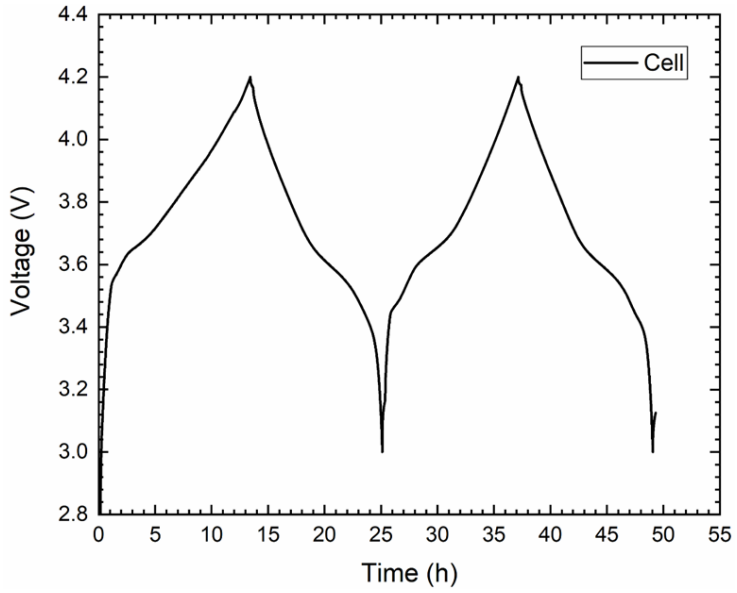

Figure 4. Voltage profile of a representative two-electrodes pouch cell acquired during the preconditioning procedure.

3.2.2 Check-up

After the preconditioning of graphite-NMC cells, a check-up procedure was performed to define the basic operation values such as the charge/discharge capacity at a higher C-rate (C/2) and the voltage values at different States of Charge (SoCs), which should resemble those reported in Table 5 of section 3.9 of deliverable D1.2. The check-up protocol was exactly the one reported in Table 8 of section 3.10 of deliverable D1.2. At the end of the check-up procedure, the charge of the cell reaches 33% of SoC. Figure 5 reports an example of the check-up procedure for a representative two-electrode pouch cell: the measured charge/discharge capacities (Ch Cap and Dch cap, respectively) are close to the nominal ones, as provided by VAR. At the 3rd GCD cycle, the voltage values at different SoCs (90, 50, 10%) are consistent with those reported in deliverable D1.2, *i.e.*, 4.0, 3.7 and 3.4 V, respectively.

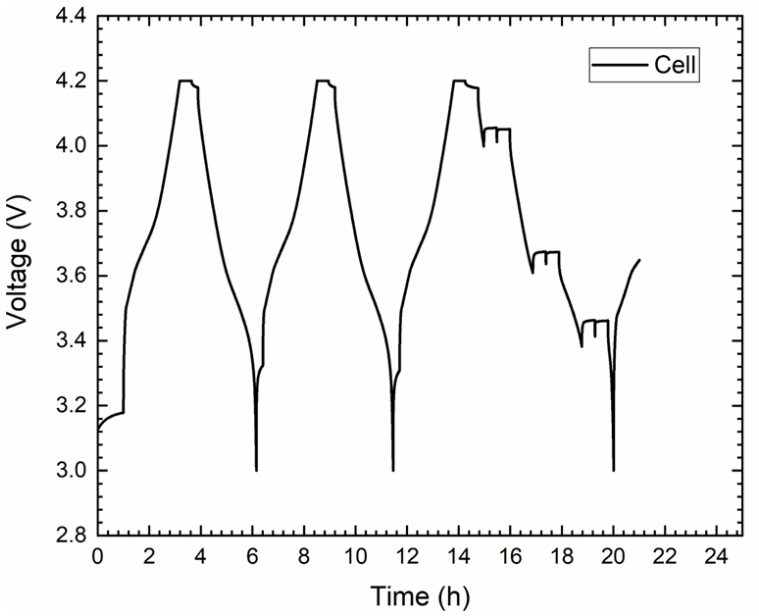

Figure 5. Voltage profile of a representative two-electrode pouch cell acquired during the check-up procedure.

3.2.3 Reference electrode stabilization

As discussed in deliverable D2.4, it is crucial to stabilize the equilibrium potential of the reference electrode to ensure reliable EIS and anode/cathode potential monitoring measurements. As described in deliverable D2.3, the equilibrium potential of the reference electrode is properly controlled when the reference electrode is brough at its 50% SoC. In the final three-electrode pouch cells, LFP-D reference electrodes were preconditioned *versus* graphite anodes, *i.e.*, by applying a GCD procedure using LFP-D as the working electrode and graphite anode as the counter electrode (NMP622 cathode was used as the reference electrode). LTO-D reference electrodes were instead preconditioned *versus* NMC cathode, *i.e.*, by applying a GCD procedure using NMC622 cathode as the working electrode and the LTO-D anode as the counter electrode (graphite was used as the reference electrode).

The applied GCD procedure was:

1) Charge at C/10 until the maximum voltage (2.7 V for LTO[5] and 3.5 for LFP[6])
2) Discharge at C/10 until 50% SoC of reference electrode (100% SoC calculated according to the theoretical capacity of the active materials)
3) Rest for 2 or 3 days

The applied current was computed considering only the capacity of the reference electrodes according to Equation (1):

$$Capacity[mAh] = \left(Weight_{RE+Celgard} - Weight_{Celgard}\right)[g] * \%AM_{RE} * \frac{S_{active\_RE}}{S_{RE}} * Theoretical\ capacity_{RE}\ [mAh\ g^{-1}] \quad (1)$$

In which $Weight_{RE+CE}$ is the weight of the 2 x 2 cm^2 reference electrode printed on Celgard®2500, $Weight_{Celgard}$ is the weight of the Celgard®2500, $\%AM_{RE}$ is the weight percentage of active material in the reference electrode (*i.e.*, 65 wt%), S_{active_RE} is the active surface of the reference electrode (strip with an area of 1.5 × 0.5 cm^2), S_{RE} is the surface of the entire reference electrode (strip with an area of 2 × 0.5 cm^2) and $Theoretical\ capacity_{RE}$ is the theoretical specific capacity of the active material of the reference electrode, *i.e.*,

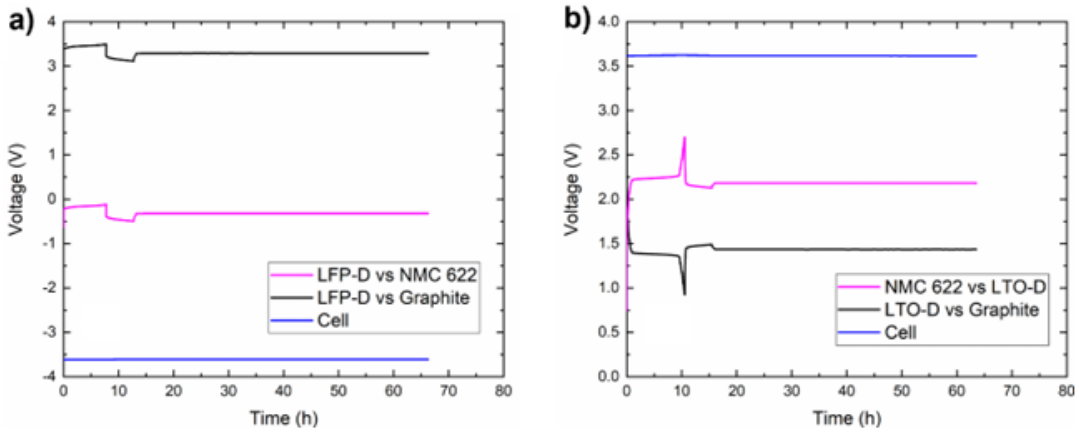

Figure 6. Voltage profiles of the pouch cells and corresponding half cells measured during the procedure for the stabilization of the investigated reference electrodes: (a) LFP-D and (b) LTO-D.

3.2.4 Galvanostatic charge/discharge cycling and electrochemical impedance spectroscopy characterization

Once stabilized, the printed reference electrodes were used to monitor the anode and cathode potentials during the galvanostatic charge/discharge cycling of the full cell, as well as to measure the impedance of the half-cell at different SoCs and Depths of Discharge (DoDs) of the full cell. To validate the reference electrode functionalities, a two-step protocol was specifically designed for the three-electrode pouch cells:

1) GCD cycles at a fixed C-rate
2) 1 GCD cycle in which EIS measurements were performed at various SoCs and DoDs of the full cell.

Potentiostatic electrochemical impedance spectroscopy (PEIS) measurements were performed with a voltage amplitude of 10 mV in a frequency range of 50 mHz - 800 kHz. Table 1 lists all the steps used for the characterization of the three-electrode pouch cells.

Table 1. List of the procedures (GCD cycles and PEIS measurements) used for the characterization of three-electrode pouch cells.

Step	Action
1	Constant current (CC) charge at 0.2C, constant voltage at maximum cell voltage*
2	CC discharge at 0.2C
3	Repeat step 2 and 3 for 9 times
4	CC charge at 0.2C until 10% of the nominal cell capacity (SoC = 10%)
5	Rest 30 min
6	PEIS at 10%
7	CC charge at 0.2C until 50% of nominal cell capacity (SoC = 50%)
8	Rest 30 min
9	PEIS at 50% SoC
10	CC charge with 0.2C until 90% of nominal cell capacity (SoC = 90%)
11	Rest 30 min
12	PEIS at 90% SoC
13	CC charge at 0.2C until maximum voltage
14	CC discharge at 0.2C until 90% of nominal cell capacity (SoC = 90%)
15	Rest 30 min
16	PEIS at 90% SoC
17	CC discharge at 0.2C until 50% of nominal cell capacity (SoC = 50%)
18	Rest 30 min
19	PEIS at 50% SoC
20	CC discharge at 0.2C until 10% of nominal cell capacity (SoC = 10%)
21	Rest 30 min
22	PEIS at 10% SoC
23	CC discharge at 0.2C until minimum cell voltage

* Constant voltage held until current below 0.02 C condition

Figure 7a and Figure 7b show the GCD measurements at C/5 for the three-electrode pouch cells using LFP-D LTO-D reference electrodes, respectively. No deviation of the anode and cathode potentials *vs.* reference electrodes were detected over time, indicating the long-term stability of the investigated reference electrodes. As shown in deliverable D2.4 and further corroborated hereafter (see Section 3.3), the presence of the reference electrodes within the cells did not affect the operation of the cell, being the electrochemical performances of the cells, measured with and without reference electrode, rather similar.

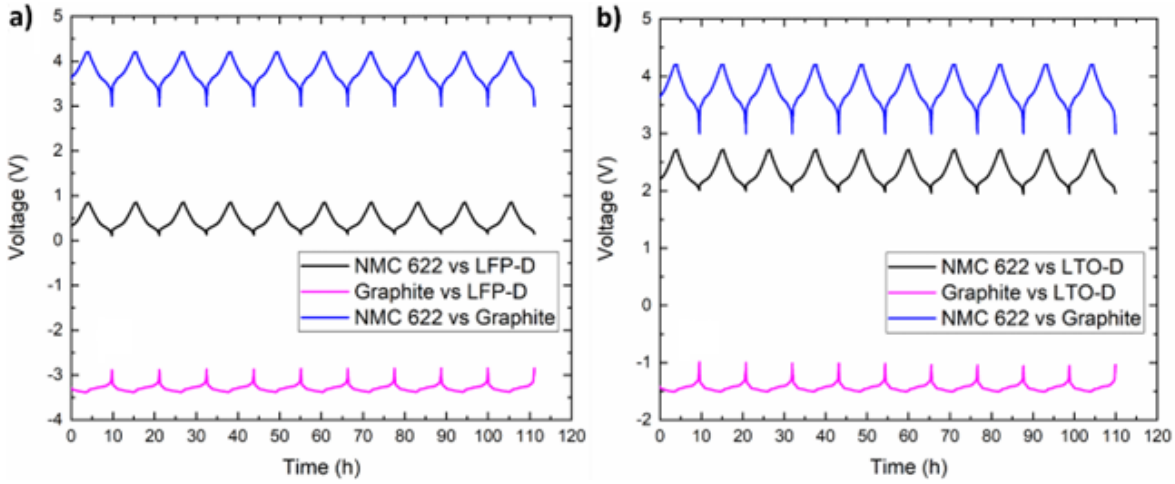

Figure 7. GCD curves at C/5 measured for the three-electrode pouch cell using the investigated reference electrodes: (a) LFP-D and (b) LTO-D.

Figure 8a and b report the GCD curves (including the rest phases where PEIS measurements were performed) measured for the three-electrode pouch cells using LFP-D and LTP-D reference electrodes, respectively, during which PEIS measurements were performed. The rest phases at various SoCs and DoDs (10%, 50% and 90%) are indicated by the dashed lines. The Ch Cap and Dch Cap were consistent with the nominal capacity (as provided by VAR) and the voltage profiles remained stable during the rest phases, confirming the stability of the reference electrodes.

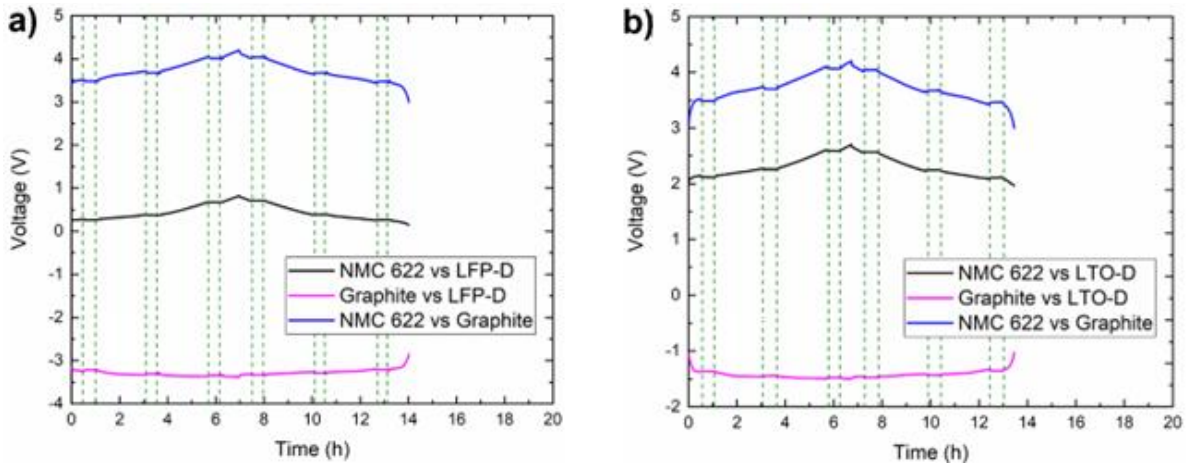

Figure 8. GCD cycle (at C/5) with rest phases where EIS measurements were acquired, measured for the three-electrode pouch cells using the investigated referent electrodes (a) LFP-D and (b) LTO-D.

Figure 9a and Figure 9b report the PEIS spectra measured for the half-pouch cell and full pouch cells using LFP-D and LTO-D reference electrodes, respectively, acquired at various SoCs and DoDs: 10% SoC, 50% SoC, 90% SoC, 10% DoD, 50% DoD, and 90% DoD.

As shown in Figure 9a-f, the PEIS data indicate that the impedance values of the pouch cell increase when the SoC decreases, especially for the impedance related to the lowest frequency semicircle, which is consistent with previous reports.[7]

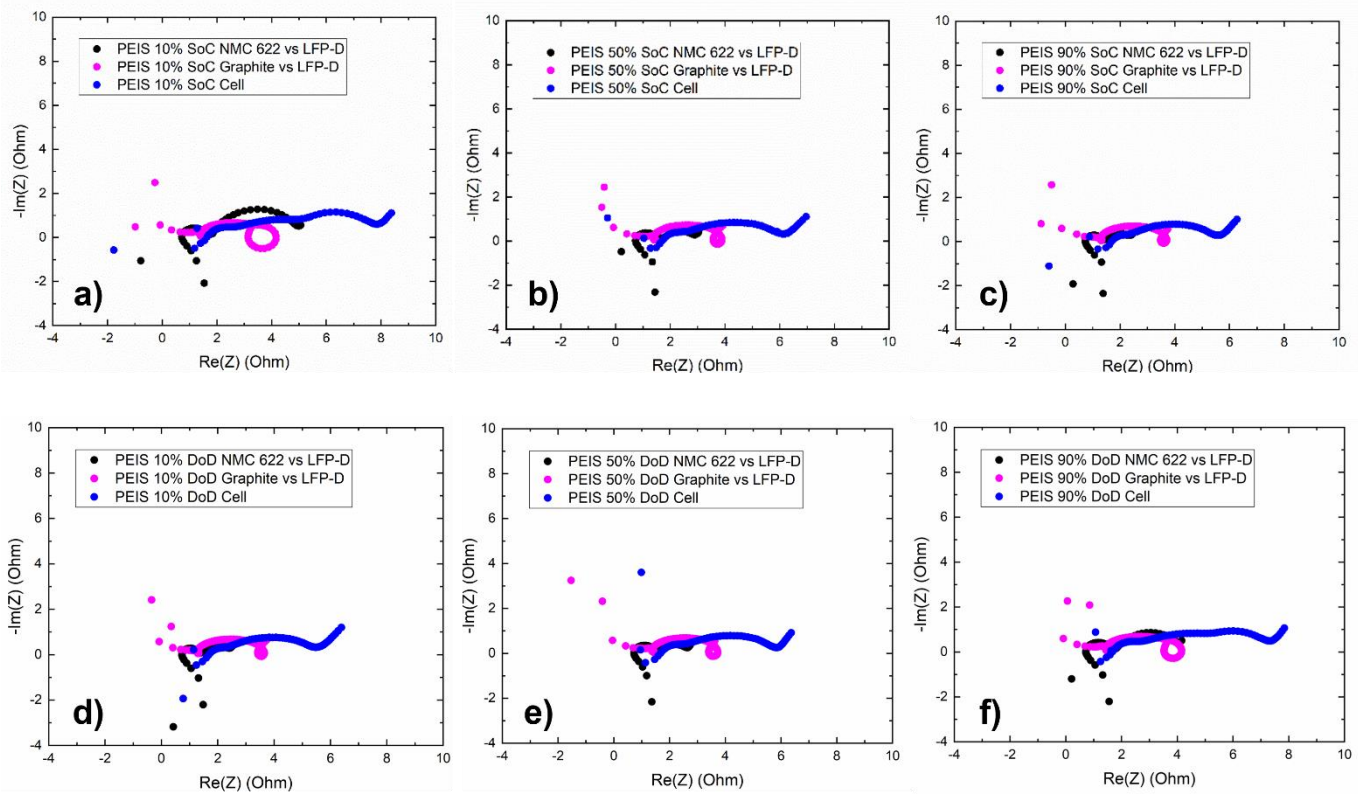

Figure 9. Nyquist plots of the half-pouch cells and full pouch cell at a)10% SoC, b) 50% SoC, c) 90% SoC, d) 10% DoD, e) 50% DoD, f) 90% DoD, measured for a representative three-electrode pouch cell configuration using an LFP-D reference electrode.

3.2.5 Final check-up

To evaluate the Ch Cap and Dch Cap of the pouch cell after the previous GCD and PEIS characterizations (step 4), the check-up procedure described in step 2 was repeated. The results are described in section 3.3 by comparing the electrochemical performance of a two-electrode pouch cell with those recorded for the three-electrode pouch cells using LFP-D or LTO-D reference electrodes.

3.3 Comparison between the performance of two- and three-electrode pouch cells

The electrochemical characterizations of two- and three-electrode pouch cells were compared to demonstrate that the insertion of a printed reference electrode does not affect the normal operation of the pouch cell.

Table 2 reports the electrochemical parameters (Ch Cap and Dch Cap and Coulombic efficiencies -CEs-) recorded for two- and three-electrode pouch cells (using LFP-D or LTO-D reference electrodes). All the cells performed 19 GCD cycles at different C rates, according to the following sequence : 1-2 preconditioning, 3-5 check-up, 6-15 GCD, 16 GCD with PEIS, 17-19 final check-up.

After the 1st cycle, in which solid electrolyte interphase (SEI) is formed, the measured CE values are higher than 95%, proving the correct operation of the pouch cells without any parasitic reactions for several GCD cycles. For cycle 6 CE values are higher than 100% due to the change of the C-rate (from C/2 to C/5) with respect to cycle 5.

For all the GCD cycles at C/5, Ch Cap and Dch cap are higher than the nominal one (2.7 mAh cm^{-2}, as provided by VAR), while they are almost equal to the nominal value for the last three GCD cycles at C/2. The Ch Cap and Dch Cap of the two-electrode pouch cell are just slightly higher than those of the three-electrode pouch cell

(capacity decrease < 6.5 %), confirming that the insertion of the reference electrode does not significantly alter the overall pouch cell operation.

Table 2. Electrochemical parameters measured for the two- and three-electrode pouch cells.

Pouch cell		Two-electrode configuration			Three electrode confirmation with LFP-D reference electrode			Three-electrode configuration with LTO-D reference electrode		
Cycle	C rate	Ch Cap	Dch Cap	CE (%)	Ch Cap	Dch Cap	CE (%)	Ch Cap	Dch Cap	CE (%)
1	C/10	3.63	3.09	85.07	3.55	2.97	83.52	3.42	2.83	82.66
2	C/10	3.18	3.15	98.90	3.04	3.00	98.74	3.01	2.97	98.88
3	C/2	3.16	3.06	96.65	3.02	2.92	96.84	3.01	2.89	95.80
4	C/2	3.05	3.05	99.91	2.92	2.91	99.78	2.90	2.88	99.25
5	C/2	3.05	3.05	100.00	2.91	2.90	99.90	2.89	2.89	99.98
6	C/5	3.07*	3.11	101.28	2.95*	2.96	100.21	2.88*	2.91	100.99
7	C/5	3.11	3.10	99.87	2.96	2.95	99.64	2.91	2.91	99.82
8	C/5	3.10	3.09	99.84	2.96	2.95	99.72	2.91	2.90	99.82
9	C/5	3.09	3.08	99.89	2.95	2.94	99.51	2.91	2.88	99.79
10	C/5	3.08	3.07	99.93	2.94	2.93	99.82	2.90	2.87	99.85
11	C/5	3.07	3.07	99.95	2.94	2.92	99.54	2.90	2.87	99.60
12	C/5	3.06	3.06	99.95	2.93	2.92	99.82	2.88	2.87	99.83
13	C/5	3.05	3.05	99.93	2.93	2.92	99.66	2.88	2.87	99.78
14	C/5	3.04	3.04	99.97	2.92	2.91	99.64	2.87	2.87	99.98
15	C/5	3.03	3.03	100.00	2.91	2.90	99.73	2.87	2.87	100.00
16	C/5	2.98	2.98	100.00	2.85	2.85	100.00	2.80	2.80	100.00
17	C/2	2.78	2.72	97.85	2.73	2.73	100.00	2.71	2.67	98.52
18	C/2	2.71	2.71	99.79	2.73	2.72	99.55	2.68	2.67	99.54
19	C/2	2.70	2.70	100.00	2.71	2.71	99.91	2.67	2.67	100.00

* Ch Cap of the 6th cycle has been computed as the sum of the Ch Cap of the 4th GCD cycle at C/2 of the check-up procedure and the Ch Cap of the 1st GCD cycle at C/5.

Finally, at different SoCs and DoDs, PEIS data measured for two-electrode pouch cell were compared with those measured for three-electrode pouch cells. The PEIS data for the latter cases were computed by summing the impedance recorded for the half-cell configurations, as shown in Figure 9.

Figure 10 reports the comparison of PEIS spectra measured for a two-electrode pouch cell and a three-electrode pouch cell using LTO-D reference electrode, at various SoCs and DoDs, as achieved through GCD cycles at C/5. For all the analysed SoCs and DoDs , the PEIS spectra for the two different pouch cell configurations are comparable. Thus, these data support that the reference electrode has marginal impedance contribution to the overall cell impedance, which is consistent with the reference electrode modelling reported in deliverable D2.4 (see also additional results in Section 3.5). The larger low-frequency impedance of the three-electrode pouch cell compared to the one of the two-electrode pouch cell could be associated to the additional reference electrode impedance, as well as to impedance discrepancies, which likely results by the assembling procedures of two different pouch cells.

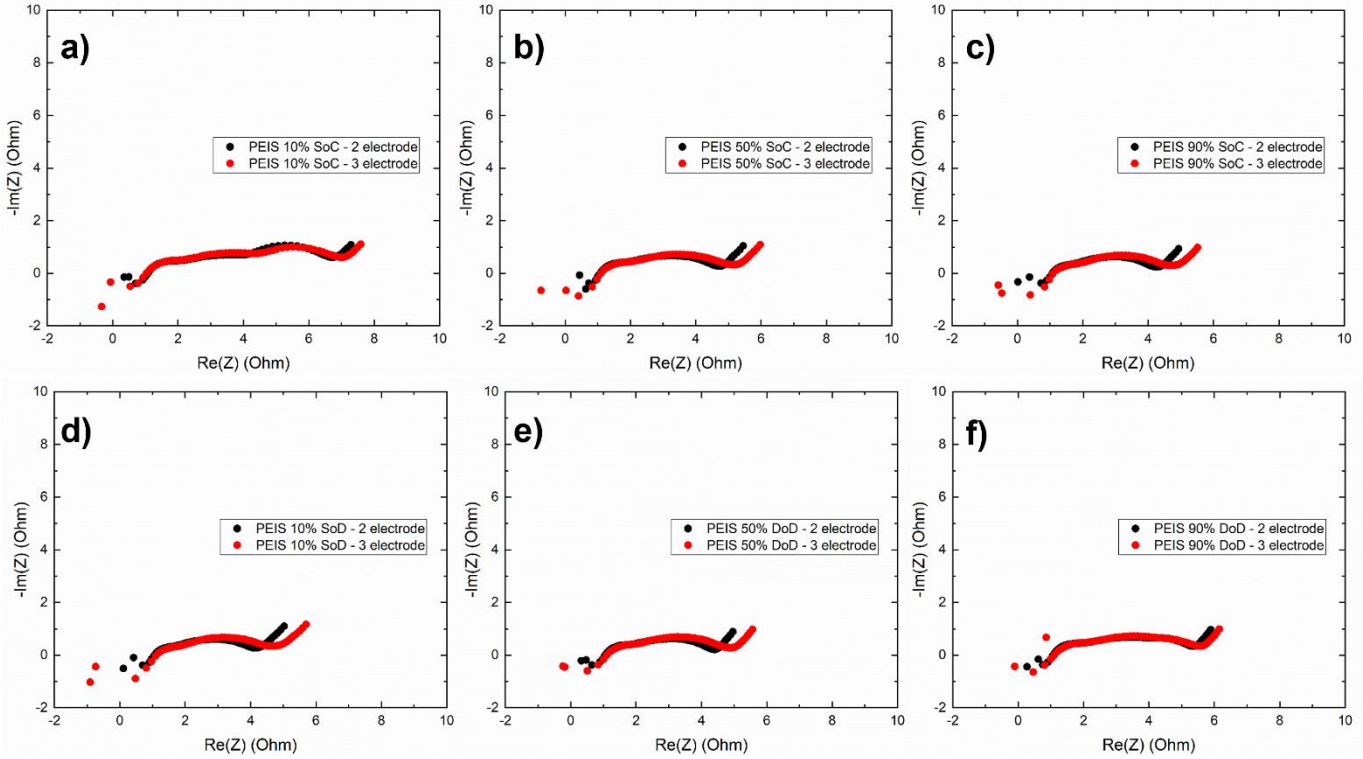

Figure 10. Nyquist plots measured for a two electrode-pouch cell and a three-electrode pouch cell using LTO-D reference electrode at various SoCs and DoDs: a)10% SoC, b) 50% SoC, c) 90% SoC, d) 10% DoD, e) 50% DoD, f) 90% DoD.

3.4 Stability of the equilibrium potential of the reference electrodes

The equilibrium potentials of the printed reference electrodes in coin cell configuration after charging at 50% SoC were monitored continuously for 400 h to confirm their long-term stability. Figure 11 shows the equilibrium potentials of representative reference electrodes during lithiation over time (400 h). The stable equilibrium potential of 3.43 V vs Li/Li^+ for LFP and 1.56 V vs Li/Li^+ for LTO-based reference electrodes are consistent with LFP[8,9] and LTO[10,11] oxidation/reduction potential values reported in literature. The equilibrium potential variation rates of the LFP-A, LFP-B, LFP-D, LTO-A, LTO-B, and LTO-D reference electrodes are as low as 79.6, 24.1, 34.2, 14.0, 14.1, and 14.4 $\mu V\ h^{-1}$, confirming the long-term stability of the reference electrodes.

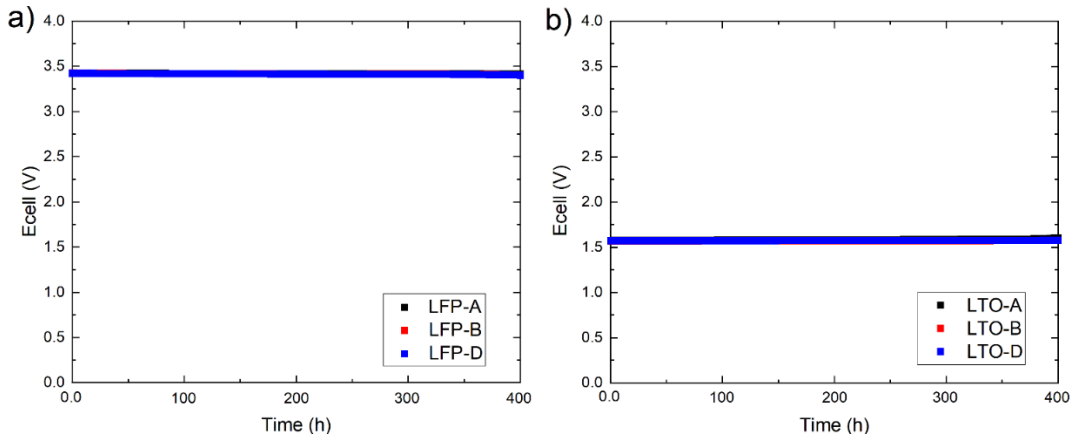

Figure 11. Equilibrium potential measurements of coin cells included reference electrodes over time after charging at 50% SoC.

3.5 Electrical modelling of the reference electrodes

As described in Section 3 of deliverable D2.4, the developed printed reference electrodes, placed between two Celgard 2500 separators, were modelled as an ultrathin (non-bulky) mesh-like electrode. Relevant parameters of the reference electrodes are the charge transfer resistance (R_{CT}), the electrolyte resistance inside the electrode pore (*e.g.*, mesh openings) (R_{EL}), and electrode characteristic time constant (given by the product between R_{CT} and the electrode capacitance -C-) (τ). Experimentally, R_{EL} can be extrapolated by measuring the high-frequency resistance of symmetric cells with stainless steel electrodes through EIS measurements. Also, R_{CT} and τ can be calculated from the EIS analysis of symmetric cells using 2 printed reference electrodes (for example, deposited on Cu or Al foil substrates to simplify the cell assembly). To extend the set of data reported in deliverable D2.4, we have performed additional characterization of the reference electrodes reducing their thickness from 50 µm to 15 µm, aiming at reducing the impedance contribution of the developed reference electrode within the pouch cells (as above characterized). Compared to the experiments reported in deliverable D2.4, an extra 0.5 mm-spacer was added in the coin cells to ensure a reproducible pressure with the electrode/separators/electrode stack. The calculated EIS impedance parameters of the investigated printed reference electrodes are reported in Table 3. Importantly, all the investigated reference electrodes exhibit a characteristic frequency (f_C) larger than > 100 kHz, and are therefore adequate to perform EIS measurements of Li-ion battery half-cells. The impedance in DC mode (Z_{DC}) of the printed reference electrodes ranges from 0.309 to 1.340 $\Omega.cm^2$, confirming that the reference electrodes add marginal series resistance contribution to the whole cell (as also corroborated by the electrochemical characterization of the pouch cells reported in the previous sections).

Table 3. Electrochemical parameters of our printed reference electrodes, extrapolated from EIS measurements.

Sample	Thickness (µm)	R_{EL} ($\Omega.cm^2$)	R_{CT} ($\Omega.cm^2$)	C ($\mu F/cm^2$)	τ (s)	f_c (kHz)	Z_{DC} ($\Omega.cm^2$)
LTO-A	~15	0.58	0.74	28.70	1.56×10^{-5}	299	0.325
LTO-B	~15	1.61	1.07	17.45	3.54×10^{-5}	190	0.642
LTO-D	~15	0.42	1.18	14.12	1.68×10^{-5}	442	0.309
LFP-A	~15	0.52	4.04	2.33	1.11×10^{-5}	2291	0.460
LFP-B	~15	0.54	4.18	2.34	1.21×10^{-5}	2173	0.478
LFP-D	~15	1.52	11.73	2.48	3.13×10^{-5}	2360	1.340

4 Conclusion

This deliverable describes the activities of Task 2.5, aiming at assessing the reliability of the printed reference electrodes in small-area (3-5 cm^2) pouch cells. To accomplish this task, LFP-D and LTO-D reference electrodes containing 65 wt% of active materials (LFP and LTO), 10 wt% of binder, and 25 wt% of conductive materials (single/few-layer graphene and carbon black) were selected for the realization of three-electrodes pouch cells with NMC622 cathode and graphite anode.

By following the general protocol reported for the final electrochemical characterization that was defined in deliverable D1.2 "Testing plan for cells and modules" containing the steps of preconditioning, check-up, reference electrode stabilization, GCD cycling at different C-rates, EIS measurements at different SoCs and DoDs, and final check-up, two and three-electrode pouch cells integrating our sensing electrodes were successfully assembled, tested, and compared. The obtained results indicate that our printed LFP-D and LTO-D reference electrodes do not alter the pouch cell operation and can be used to accurately monitor distinctively the potentials of the battery electrodes, as well as to perform reliable EIS measurements of the half cells. The investigated reference electrodes have shown stable equilibrium potentials, around the oxidation/reduction potentials of their active materials (*i.e.*, 3.45 V for LFP and 1.55 V for LTO), over 400 h, ensuring the long-term operation in practical applications. Based on the electrical modelling reported in deliverable D2.4, we have confirmed that the reference electrode used in the three-electrode pouch cells exhibit f_C larger than 100 kHz, meeting the specifications requested for the EIS analysis of Li-ion battery half cells.

5 Risks

Risk No.	What is the risk	Probability of risk occurrence[1]	Effect of risk[2]	Solutions to overcome the risk
WP2.1	*Low reproducibility of coin cells including reference electrodes*	*3*	*2*	*Optimization of the electrolyte amount and spacer thickness*

[1] Probability risk will occur: 1 = high, 2 = medium, 3 = Low

[2] Effect when risk occurs: 1 = high, 2 = medium, 3 = Low

6 References

1 T. Kim, W. Choi, H.-C. Shin, J.-Y. Choi, J. M. Kim, M.-S. Park and W.-S. Yoon, *J. Electrochem. Sci. Technol*, 2020, 11, 14–25.

2 N. Delaporte, D. B. Ossonon, K. Zaghib and D. Bélanger, *Batter. Supercaps*, 2020, 3, 638–646.

3 X. Sun, P. V Radovanovic and B. Cui, *New J. Chem.*, 2015, 39, 38–63.

4 S.-P. Chen, D. Lv, J. Chen, Y.-H. Zhang and F.-N. Shi, *Energy & Fuels*, 2022, 36, 1232–1251.

5 D. Farhat, D. Lemordant, J. Jacquemin and F. Ghamouss, *J. Electrochem. Soc.*, 2019, 166, A3487.

6 J. Jiang, W. Shi, J. Zheng, P. Zuo, J. Xiao, X. Chen, W. Xu and J.-G. Zhang, *J. Electrochem. Soc.*, 2014, 161, A336.

7 V. J. Ovejas and A. Cuadras, *Batteries*, 2018, 4.

8 B. Rowden and N. Garcia-Araez, *Energy Reports*, 2021, 7, 97–103.

9 M. J. Loveridge, M. J. Lain, I. D. Johnson, A. Roberts, S. D. Beattie, R. Dashwood, J. A. Darr and R. Bhagat, *Sci. Rep.*, 2016, 6, 37787.

10 X. Shi, S. Yu, T. Deng, W. Zhang and W. Zheng, *J. Energy Chem.*, 2020, 44, 13–18.

11 R. Fu, X. Zhou, H. Fan, D. Blaisdell, A. Jagadale, X. Zhang and R. Xiong, *Energies*, 2017, 10.

12 J. Hou, R. Girod, N. Nianias, T.-H. Shen, J. Fan and V. Tileli, *J. Electrochem. Soc.*, 2020, 167, 110515.

7 Acknowledgement

The author(s) would like to thank the partners in the project for their valuable comments on previous drafts and for performing the review.

Project partners

#	PARTICIPANT SHORT NAME	PARTNER ORGANISATION NAME	COUNTRY
1	IKE	IKERLAN S. COOP.	Spain
2	BDM	BEDIMENSIONAL SPA	Italy
3	POL	POLITECNICO DI TORINO	Italy
4	FHG	FRAUNHOFER GESELLSCHAFT ZUR FOERDERUNG DER ANGEWANDTEN FORSCHUNG E.V.	Germany
5	FM	FLANDERS MAKE VZW	Belgium
6	TUE	TECHNISCHE UNIVERSITEIT EINDHOVEN	The Netherlands
7	NXP NL	NXP SEMICONDUCTORS NETHERLANDS BV	The Netherlands
8	NXP FR	NXP SEMICONDUCTORS FRANCE SAS	France
9	ABEE	AVESTA BATTERY & ENERGY ENGINEERING	Belgium
10	VAR	VARTA INNOVATION GMBH	Germany
11	AIT	AIT AUSTRIAN INSTITUTE OF TECHNOLOGY GMBH	Austria
12	UNR	UNIRESEARCH BV	The Netherlands

DISCLAIMER/ ACKNOWLEDGMENT

This project has received funding from the European Union's Horizon 2020 research and innovation programme under grant agreement No 957273. The information and views set out in this publication does not necessarily reflect the official opinion of the European Commission. Neither the European Union institutions and bodies nor any person acting on their behalf, may be held responsible for the use which may be made of the information contained therein.